Journal of Global Change Data & Discovery. 2025, 9(3): 262-278
www.geodoi.ac.cn


# Spatial Analysis Method for Risk Areas and Rescue Accessibility of High-voltage Power Towers: a Case Study of Guangzhou City, China

Liu, C.[1,2] Yang, Y.[3] Li, S. J. [4] He, Y. L.[5] Yang, Z.[5] Wang, S. H.[1,2*]

1. State Key Laboratory of Remote Sensing and Digital Earth, Aerospace Information Research Institute, Chinese Academy of Sciences, Beijing 100101, China;
2. University of Chinese Academy of Sciences, Beijing 100049, China;
3. China Southern Power Grid Digital Platform Technology Company, Shenzhen 518100, China;
4. China Southern Power Grid Company Limited, Guangzhou 510663, China;
5. Faculty of Geomatics, Lanzhou Jiaotong University, Lanzhou 730070, China

**Abstract:** Electric power infrastructure is a crucial guarantee for production and daily life. High-voltage power grids are spread throughout the city, and high-voltage power towers are important nodes in the power network. Collapse accidents often occur, and in the event of an accident, emergency response from fire rescue is required. This study takes Guangzhou City as an example, comprehensively collects the data of the spatial distribution of high-voltage power towers, and utilizes the spatial analysis method of Geographic Information System (GIS). By analyzing the buffer zones of high-voltage power towers, roads and buildings, overlaying them to produce the adjacent risk areas, and calculating the fire rescue accessibility of high-voltage power towers, we propose a comprehensive spatial analysis method for calculating the risk areas and rescue accessibility of high-voltage power towers. The analysis process includes the statistics of the number of high-voltage power towers, the delineation of the spatial distribution of high-voltage power tower risk areas, the calculation of fire rescue time, and the calculation of fire rescue accessibility. Among them, the delineation process of high-voltage power tower risk areas includes the delineation of road-near risk areas, building-near risk areas, and comprehensive risk areas, as well as the calculation of area with risk areas and population in risk areas. This method provides a reference for the rescue operation of high-voltage power tower collapse accidents and the resilience construction of megacities.

**Keywords: power tower; spatial analysis; risk area; accessibility; Guangzhou**

**DOI:** https://doi.org/10.3974/geodp.2025.03.02

## 1 Introduction

As a core component of the urban lifeline system, power infrastructure is an important guarantee for production and life, and it is the “energy bloodline” that sustains the economic

**Received:** 08-06-2025; **Accepted:** 29-08-2025; **Published:** 25-09-2025

**Foundations:** China Southern Power Grid Company Limited (ZBKJXM20240174); Chinese Academy of Sciences (E43302020D, E2Z105010F)

*__Corresponding Author:__ Wang, S. H., Aerospace Information Research Institute, Chinese Academy of Sciences, wangshaohua@aircas.ac.cn

**Citation:** Liu, C., Yang, Y., Li, S. J., *et al*. Spatial analysis method for risk areas and rescue accessibility of high-voltage power towers: a case study of Guangzhou City, China [J]. *Journal of Global Change Data & Discovery*, 2025, 9(3): 262–278. https://doi.org/10.3974/geodp.2025.03.02.

operation of modern society[1]. The United Nations Sustainable Development Goal 9 clearly states that it is necessary to build high-quality, reliable, sustainable and disaster-resilient infrastructure[2]. As an important infrastructure, the construction of high-voltage transmission grids is of great significance[3]; High-voltage lines and transmission towers, as the edges and nodes of the power grid, jointly form the high-voltage transmission network. As the most important existing power dataset, OpenStreetMap data stores relatively comprehensive structured power network information, and some researchers have also conducted relatively comprehensive studies based on this data source[4].

As nodes of high-voltage transmission networks, the significance of high-voltage transmission towers cannot be underestimated. Their safety not only determines the stability of daily power supply but also supports the industrial and commercial production of cities and the living security of millions of people[5]. High-voltage power towers have to withstand the pressure of numerous events such as storms, karst conditions, and construction, so under the circumstances of typhoons, thunderstorms, and geological disasters, they are highly prone to collapse accidents, posing a significant risk to the lives and property of the surrounding residents[6–9]. The inspection of power transmission grids and high-voltage power towers through aerial remote sensing images under adverse weather conditions plays a significant role in the construction of smart grids, promoting the development of remote sensing technology for identifying and extracting power towers[10,11].

With the gradual acceleration of urbanization, the density of urban power grids has soared. Many power towers are laid along roads or suspended above buildings, posing a significant safety hazard to the city. Once high-voltage power towers collapse, they will pose a threat to the lives and property of pedestrians, vehicles, and residents[12]. Once an electric tower collapses, apart from directly affecting vehicles, pedestrians and building facilities, it is highly likely to cause secondary hazards such as fires[13]. Therefore, the efficiency and accessibility of emergency rescue after an accident are important guarantees for the safety of the surrounding residents and the restoration of the power system[14].

As a super-large city on the southeast coast of the subtropical zone in China, Guangzhou is not only confronted with the threat of extreme weather caused by climate change, but also has the spatial characteristics of dense population and complex functions. Coupled with its coastal terrain that is high in the northeast and low in the southwest, it poses higher requirements for the safety and resilience of transmission towers[15]. The existence of risk areas not only may lead to power outages, but also, due to the spatial conflicts between power towers and roads and buildings, will block post-disaster rescue channels and delay the progress of emergency repairs. GIS has powerful spatial analysis capabilities. By using computers to analyze raw data and digital maps, new cognitive and decision-making bases can be obtained, and it has been widely applied in various related fields[16,17]. Analyzing the distribution of risk areas between transmission towers and adjacent roads and buildings, and calculating the accessibility of fire safety rescue for high-voltage power towers, is not only a requirement for ensuring the safety of the power system itself, but also a core support for building an urban disaster emergency response system and enhancing post-disaster recovery capabilities, providing key technical references for the resilience construction of megacities.

## 2 Data Sources and Analysis Methods

### 2.1 Data Sources

The spatial distribution data of high-voltage power towers is derived from the open-source map database OpenStreetMap (OSM)[1], obtained by querying the “tower” nodes under the

[1] OpenStreetMap. https://www.openstreetmap.org.

"power" layer through the Overpass Query Language (OverpassQL) interface, exported in GeoJSON format and converted to Shapefile in ArcGIS Pro 3.0 software[18]. Take Guangzhou City as an example. The high-voltage power tower data covers 11 districts of Guangzhou City, with a total of 15,375 points.

The boundaries of administrative divisions are derived from the National Catalogue Service for Geographic Information[2]; The road data is also sourced from the open-source map database OSM; The building data is derived from the data paper of Zhang, *et al*.[19]; The population raster data is derived from the data paper by Chen, *et al*.[20]; The data of the fire station is sourced from the Amap Open Platform[3]. The above vector data is in the WGS1984 coordinate system, and the population raster data is in the Albers equal-area conic projection.

## 2.2 Spatial Analysis Method

### 2.2.1 Buffer and Overlay Analysis Methods

The buffer zone is a transitional zone for mitigating external risks of geographical entities, and it is a polygonal area of a certain width formed around the geographical entity[21]. Buffer zone analysis is one of the important spatial analysis methods in GIS, and its main purpose is to determine the service or influence range of geographical entities. The buffer analysis method takes the boundaries of points, lines, and polygons as the center and creates a buffer polygon within a specified distance around the input feature[22]. Overlay analysis is a spatial analysis method that overlays different vector graphics layers in the same area to perform graphic and attribute operations, generating new spatial graphics within the same range[23]. The intersection analysis of polygons extracts the common areas of different polygons, and the new polygon generated is the intersection of the original polygon; the combination or joint analysis of polygons generates the common range of all polygons, and the new polygon produced is the union of the original polygons[24].

During the analysis process, a point buffer zone of corresponding distance was created with the high-voltage power tower point as the center (Figure 1a), and the high-risk area around the high-voltage power tower was determined as the risk area of the high-voltage power tower. Establish line buffer zones (Figure 1b) and polygon buffer zones (Figure 1c) at corresponding distances for roads and buildings respectively. Intersect the risk areas of high-voltage power towers with the buffer zones of roads and buildings respectively (Figure 2a and Figure 2b), forming risk areas adjacent to roads and buildings. The road-adjacent risk area and the building-adjacent risk area are superimposed (Figure 2c) and combined to obtain the comprehensive risk area. The 3 types of risk areas are respectively intersected with administrative divisions to obtain the area and proportion of risk areas in each administrative region. Finally, it is superimposed with the population grid, and the population covered by the risk area is obtained by using spatial statistical methods[25].

a. Point buffer of towers b. Line buffer of roads c. Polygon buffer of buildings

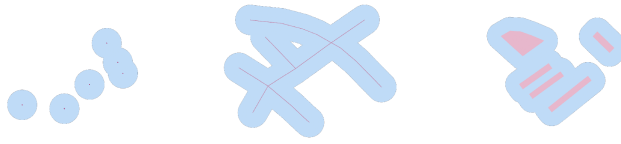

**Figure 1** Example of the feature buffer

[2] National Catalogue Service for Geographic Information. https://www.webmap.cn/main.do?method=index.

[3] Amap Open Platform. https://lbs.amap.com/.

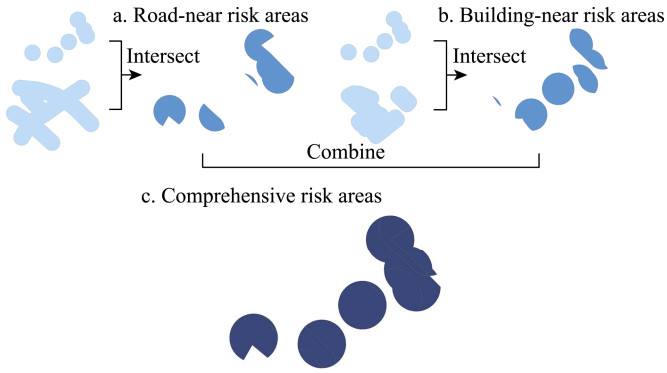


**Figure 2** Example of buffer overlay

### **2.2.2** Accessibility Calculation Method

Accessibility refers to the quantitative expression of the ease or expectation of people overcoming obstacles such as distance or time to reach service facilities or activity venues[26]. Temporal accessibility mainly considers the travel time from the supplier to the demand side, while spatial accessibility emphasizes the spatial relationship between the supplier and the demand side. Network analysis method and two-step floating catchment area method are the most common methods for calculating accessibility[27]. The network analysis of the nearest facility method to calculate the travel time only studies from the supply perspective when a single fire station can reach the high-voltage power tower; the two-step floating catchment area method takes into account both supply and demand aspects to calculate the number of fire stations that can be obtained from high-voltage power towers in the event of simultaneous accidents[28].

The urban road network serves as the framework and carrier of urban social and economic activities, and it is the core link of fire rescue operations[29]. The network analysis method builds a network dataset based on the urban road network, and conducts calculations by taking high-voltage power towers and fire stations as event points and facility points respectively. Calculate the nearest facility point to obtain the shortest rescue time for each high-voltage power tower; and calculate the OD cost matrix to obtain the network travel time between each fire station and each high-voltage power tower[30].

The two-step floating catchment area method conducts 2 searches centered on the supply point (in this study, the fire station) and the demand point (in this study, the high-voltage power tower) within the determined range, and calculates the available supply (number of facilities) at the demand point[31]. The Gaussian floating catchment area method introduces a Gaussian attenuation function to replace the fixed radius without distance attenuation, and performs distance attenuation in 2 searches[32]. During the analysis process, considering the actual driving conditions of the fire engine, the network distance (network travel time) was used to replace the planar Euclidean distance, and the OD cost matrix of the network analysis method was introduced for calculation[33].

The first step is to calculate the supply-demand ratio for each fire station:

$$R_i = \frac{S_i}{\sum_{j\epsilon\left\{t_{ij}\le t_0\right\}} D_j G\left(t_{ij}\right)} \tag{1}$$

where, $R_i$ represents the supply-demand ratio of fire station $i$. $S_i$ represents the total service capacity of fire station $i$. Here, it is assumed that the total service capacity of each fire station is the same and is set to 1. $t_{ij}$ is the driving time from fire station $i$ to high-voltage power tower $j$, and $t_0$ is the search time threshold of the service area. $D_j$ represents the

demand of the high-voltage power tower $j$. Here, it is assumed that the demand of each high-voltage power tower is 1. $G\left(t_{ij}\right)$ is the Gaussian decay function:

$$G\left(t_{ij}\right)=\frac{e^{-\frac{1}{2}\times\left(\frac{t_{ij}}{t_0}\right)^2}-e^{-\frac{1}{2}}}{1-e^{-\frac{1}{2}}} \tag{2}$$

For each determined fire station $i$, a time scope is formed based on the maximum search time $t_0$. Search for high-voltage power towers that fall within the time domain in the OD cost matrix and calculate the weighted quantity using the Gaussian attenuation function. The supply-demand ratio of fire station $i$ is obtained by dividing the total service capacity of the fire station by the weighted demand quantity.

The second step is to calculate accessibility for each high-voltage power tower:

$$Acc_j=\sum_{i\epsilon\left\{t_{ij}\le t_0\right\}}R_iG\left(t_{ij}\right) \tag{3}$$

where, $Acc_j$ represents the accessibility of each high-voltage power tower $j$, which is the total amount of fire station services obtained.

For each high-voltage power tower $j$, a time scope is also formed based on the maximum search time $t_0$. Search for fire stations within this time scope in the OD cost matrix, use the Gaussian attenuation function to weight the supply and demand ratio, and add them up to obtain the accessibility of each high-voltage power tower $j$, that is, the number of fire rescue facilities that each high-voltage power tower can be allocated within a certain range.

### 2.3 Technical Approach

The spatial analysis process of risk areas and rescue accessibility for high-voltage power towers mainly takes high-voltage power tower, road, building, and fire station as the basic data. It delineates the adjacent risk areas of high-voltage power towers, calculates the fire rescue time and accessibility. The technical route of the analysis process is shown in Figure 3, and the specific steps are as follows:

(1) Collect basic data such as high-voltage power towers, administrative divisions, roads, buildings, population, and fire stations, unify the coordinate systems of the data, and convert the coordinate systems of the data into the WGS1984 geographic coordinate system and the UTM projection coordinate system;

(2) Explore the spatial distribution of high-voltage power towers and count the number of high-voltage power towers in each area;

(3) Create a 50-m buffer zone around the high-voltage power tower as a high-risk area. At the same time, create 50-m buffer zones for roads and buildings. Intersect the 50-m buffer zones of the high-voltage power tower with those of roads and buildings respectively to obtain the risk areas adjacent to roads and buildings. Combine the 2 types of risk areas to obtain a comprehensive risk area;

(4) Calculate the area of various risks in each district and the population covered by risk areas in each district;

(5) Based on the geographical locations of the existing fire stations, calculate the rescue time required from the nearest fire station to each high-voltage power tower through the road network;

(6) Calculate the rescue time from each fire station to each high-voltage power tower as

the OD cost matrix. Through the Gaussian attenuation function and time threshold, calculate the fire rescue accessibility of each high-voltage power tower using the two-step floating catchment area method.

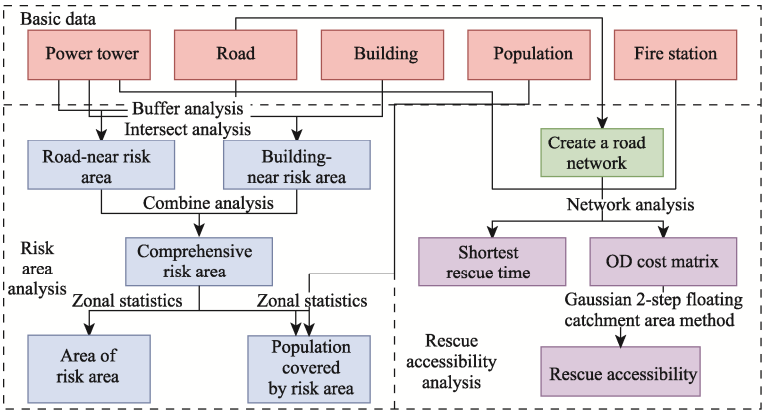


**Figure 3** Flowchart of the spatial analysis

## 3 Case Analysis Results

### 3.1 Analysis Result Data Overview

The spatial analysis process of risk areas and rescue accessibility for high-voltage power towers mainly generates results such as high-voltage power tower point data (PowerTower), high-voltage power tower adjacent risk area data (RiskArea), high-voltage power tower rescue time (RescueTime), and high-voltage power tower rescue accessibility (RescueAccessibility). Among them, the risk area data include risk areas adjacent to roads, risk areas adjacent to buildings, and comprehensive risk areas; the rescue time and rescue accessibility results are archived in the form of attribute tables in the high-voltage power tower point data; the fields included in the high-voltage power tower point data and the meanings and descriptions they represent are shown in Table 1.

**Table 1** The field list of the power tower point data

| Field name | Content | Description |
|---|---|---|
| ID | Number | The power tower number in this study |
| OSMID | Number in OSM | The power tower number in OSM |
| Province/ProvinceCN | Province | The provincial-level administrative region to which the power tower belongs |
| City/CityCN | City | The prefecture-level administrative region to which the power tower belongs |
| District/DistrictCN | District | The county-level administrative region to which the power tower belongs |
| Adcode | Administrative code | The county-level administrative code to which the power tower belongs |
| Longitude | Longitude | The longitude geographical coordinates of the power tower |
| Latitude | Latitude | The latitude geographical coordinates of the power tower |
| TimeOF | Rescue time | The shortest driving time from the fire station to the power tower |
| Accessibility5 | 5-minute accessibility | The accessibility of fire stations with a time threshold of 5 minutes |
| Accessibility10 | 10-minute accessibility | The accessibility of fire stations with a time threshold of 10 minutes |
| Accessibility15 | 15-minute accessibility | The accessibility of fire stations with a time threshold of 15 minutes |
| Accessibility30 | 30-minute accessibility | The accessibility of fire stations with a time threshold of 30 minutes |

### 3.2 Case Study of Guangzhou City

**3.2.1** Spatial Distribution and Statistical Data Calculation of Power Towers

The spatial analysis process first requires collecting all high-voltage power towers in the study area from the open-source map database OpenStreetMap, which spatial distribution is shown in Figure 4. There is a total of 15,375 high-voltage power towers in Guangzhou City. By overlaying the power tower data of each district with the administrative division data, the number of power towers in each district is statistically calculated as shown in Figure 5. The number of power towers in each section varies greatly. The different locations, sizes and land use methods of each administrative district result in variations in the number of power towers: the administrative districts in the city center are small in area and have relatively complete underground cable laying, thus having a lower demand for ground power towers; the area of the peripheral counties and districts is relatively large, and more power towers are needed to cover large areas to ensure power supply.


**Figure 4** Spatial distribution map of high-voltage power towers in Guangzhou

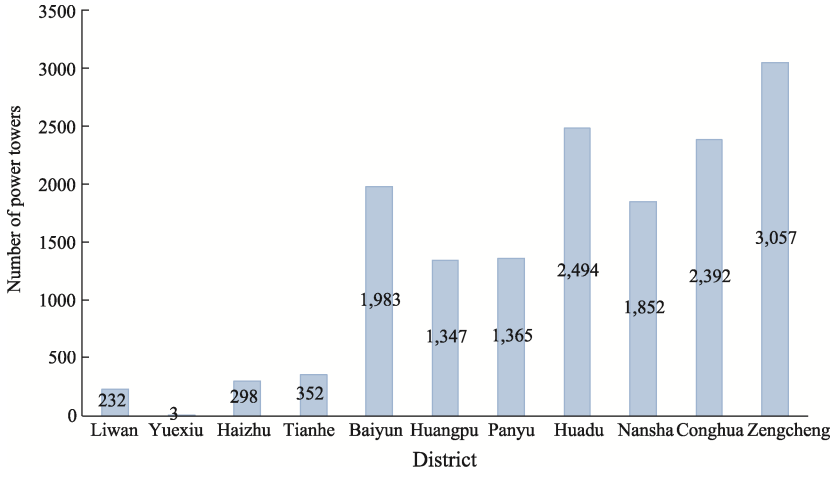


**Figure 5** Statistical of the number of power towers in various districts of Guangzhou

**3.2.2** Demarcation of Road-near Risk Areas for High-voltage Power Towers

Create a 50-m buffer zone for the high-voltage power towers in the study area as a high-risk zone around the high-voltage power towers. A 50-m buffer zone was created for the roads

within the study area and intersected with the 50-m buffer zone of the high-voltage power tower to form a risk area adjacent to the roads of the high-voltage power tower (Figure 6). The area of road-near risk zones within each administrative region and the proportion of risk zones in the total administrative region are statistically analyzed, as shown in Table 2 and Figure 7. The total area of the risk zones near to roads is 38.825 km$^2$. The risk zones in the peripheral counties are larger, but the proportion of risk zones in Liwan, Haizhu, Tianhe and other districts is even larger, highlighting the planning conflict between the historical road network in the old urban area and the safety distance of power towers.

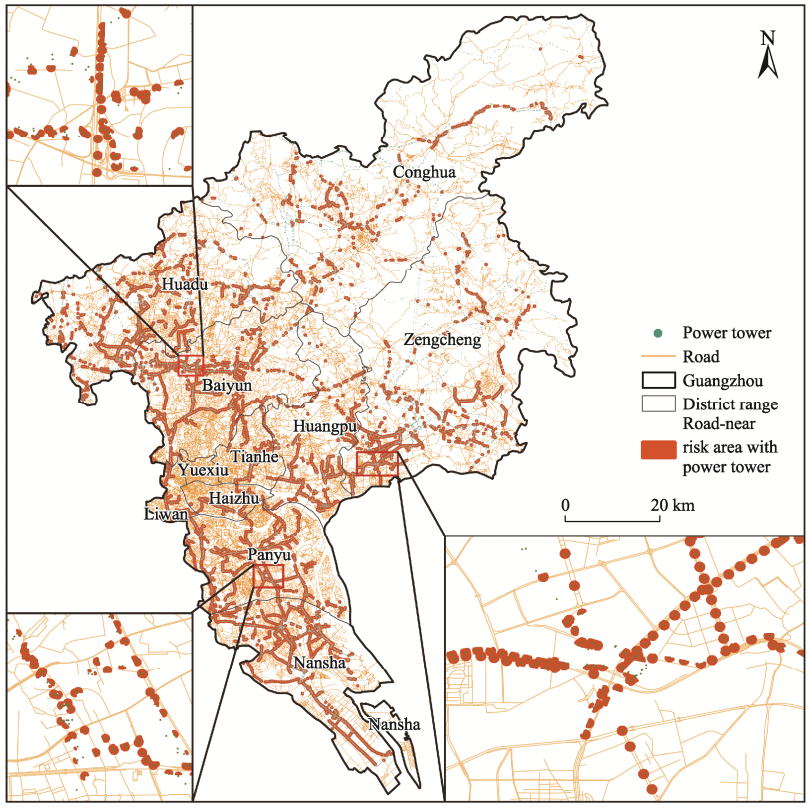


**Figure 6** Spatial distribution map of road-near risk areas in Guangzhou

**Table 2** Statistical of the area of road-near risk areas in Guangzhou

| District | Area of the risk zone (m$^2$) | Proportion (%) |
|---|---|---|
| Liwan | 968,716 | 1.55 |
| Yuexiu | 23,349 | 0.07 |
| Haizhu | 1,210,462 | 1.31 |
| Tianhe | 1,372,059 | 1.01 |
| Baiyun | 5,411,325 | 0.81 |
| Huangpu | 4,309,663 | 0.89 |
| Panyu | 4,865,572 | 0.94 |
| Huadu | 6,541,263 | 0.68 |
| Nansha | 6,098,480 | 0.92 |
| Conghua | 2,071,853 | 0.10 |
| Zengcheng | 5,952,504 | 0.37 |
| Guangzhou | 38,825,246 | 0.54 |

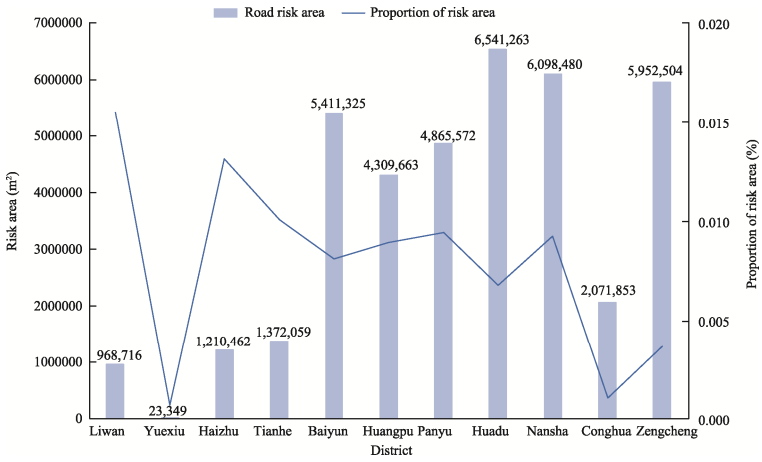


**Figure 7** Statistical of the area of road-near risk areas in Guangzhou

### **3.2.3** The Demarcation of Building-near Risk Areas for High-voltage Power Towers

A 50-m buffer zone was also created for the building outlines within the study area and intersected with the 50-m buffer zone of the high-voltage power tower to form a risk area adjacent to the buildings of the high-voltage power tower. The spatial distribution is shown in Figure 8. The area of building-near risk zones within each administrative region and the proportion of risk zones in the total administrative region were statistically analyzed, as shown in Table 3 and Figure 9. The total area of the risk zone near to buildings is 16.035 $km^2$, and the proportion of the area near the old urban area, especially in Liwan District, is relatively high. The planar blue patches in the old urban area, the cluster distribution of urban villages, and the scattered points in the new district directly present the spatial gradient of the risk area.

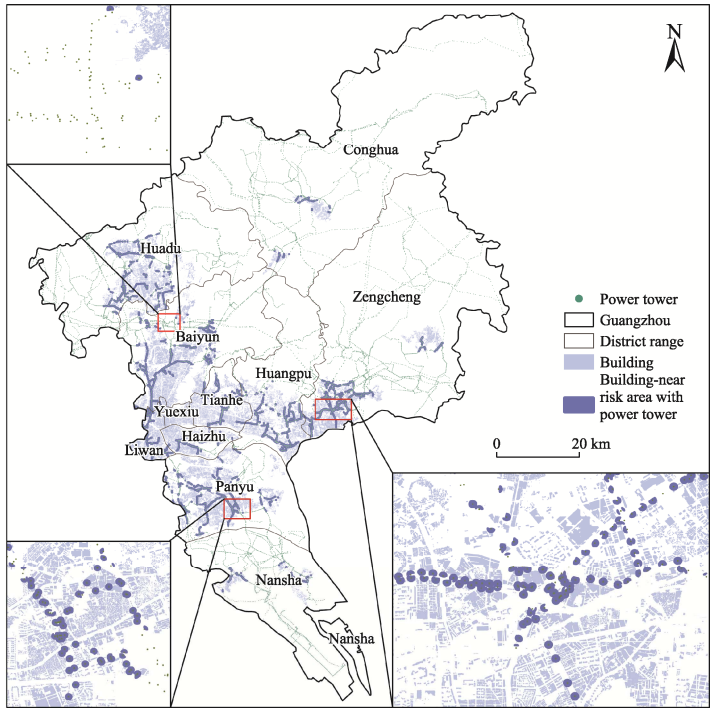


**Figure 8** Spatial distribution map of building-near risk areas in Guangzhou

**Table 3** Statistical of the area of building-near risk areas in Guangzhou

| District | Area of the risk zone ($m^2$) | Proportion (%) |
|---|---|---|
| Liwan | 1,275,287 | 2.04 |
| Yuexiu | 22,865 | 0.07 |
| Haizhu | 838,624 | 0.91 |
| Tianhe | 1,160,680 | 0.85 |
| Baiyun | 2,817,368 | 0.42 |
| Huangpu | 1,968,870 | 0.41 |
| Panyu | 2,462,211 | 0.48 |
| Huadu | 2,163,910 | 0.22 |
| Nansha | 374,290 | 0.06 |
| Conghua | 286,118 | 0.01 |
| Zengcheng | 2,664,819 | 0.16 |
| Guangzhou | 16,035,043 | 0.22 |

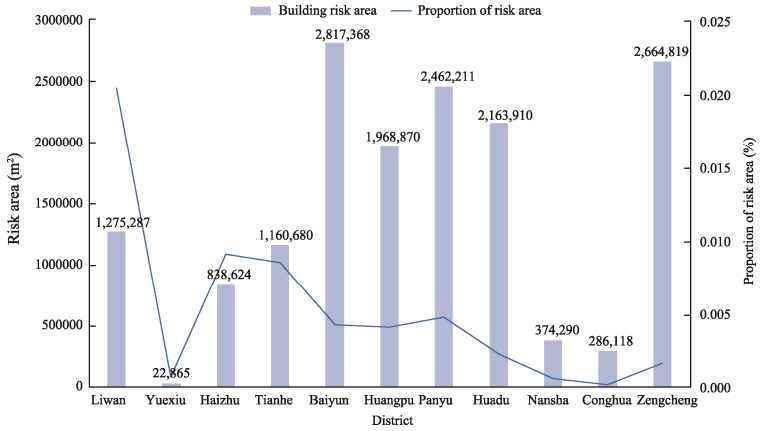


**Figure 9** Statistical of the area of building-near risk areas in Guangzhou

**3.2.4** The Demarcation of Comprehensive Risk Areas for High-voltage Power Towers

Combine the road-near risk area and the building-near risk area to obtain the comprehensive risk area, and the spatial distribution is shown in Figure 10. The area of comprehensive risk zones within each administrative region and the proportion of risk zones in the total administrative region are statistically analyzed, as shown in Table 4 and Figure 11. The total area of comprehensive risk zones in Guangzhou City is 44.255 $km^2$. Urban areas such as Liwan, Haizhu and Tianhe have small administrative regions and a small number of power towers, but the proportion of risk areas is high. The peripheral districts such as Huadu, Nansha and Zengcheng cover a vast area and have a large number of power towers, forming a large area of risk zones.

**3.2.5** Analysis of the Population Covered in the Risk Area of Power Towers

The population within the comprehensive risk area was statistically divided by adminstrative region, and the proportion of the risk population (the proportion of the population in the risk area to the total population of the region area) was calculated. The statistical results are shown in Table 5 and Figure 12. From the perspective of the population size in risk areas, the geographical distribution shows a significant imbalance. The population in the risk area of Huadu District is the largest, reaching 63,239. Panyu District follows closely with 41,712, followed by Huangpu District (22,878 persons), Nansha District (18,503 persons), and Zengcheng District (18,212 persons). The population in the risk area of Yuexiu District is the smallest, with only 544 persons. Liwan District (4,600 persons) and Tianhe District (7,660 persons) are also at a relatively low level.

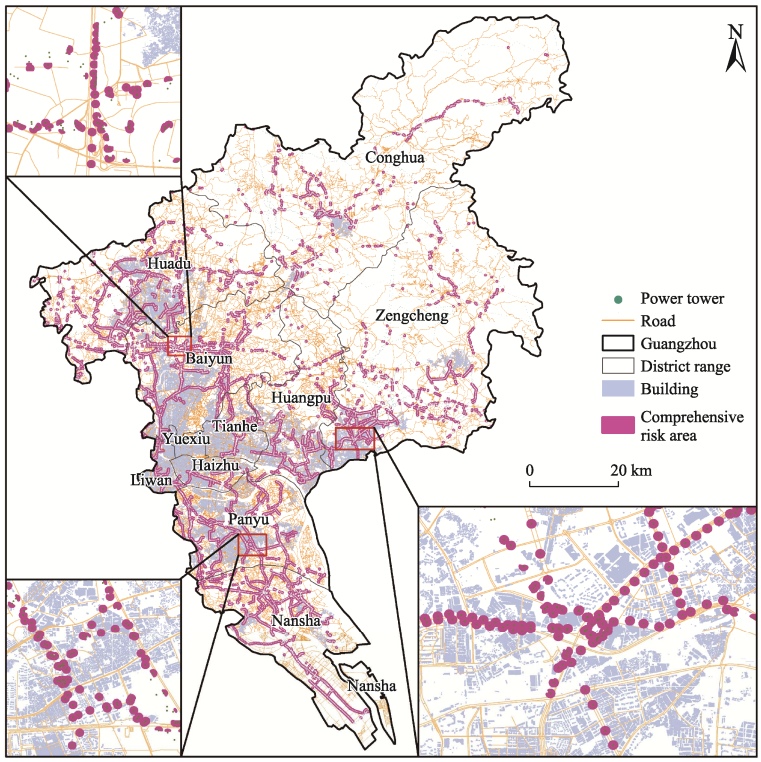


**Figure 10** Spatial distribution map of comprehensive risk areas in Guangzhou

**Table 4** Statistical of the area of comprehensive risk areas in Guangzhou

| District | Area of the risk zone ($m^2$) | Proportion (%) |
|---|---|---|
| Liwan | 1,439,851 | 2.31 |
| Yuexiu | 23,352 | 0.07 |
| Haizhu | 1,399,563 | 1.52 |
| Tianhe | 1,750,761 | 1.29 |
| Baiyun | 6,533,528 | 0.98 |
| Huangpu | 4,953,379 | 1.03 |
| Panyu | 5,914,622 | 1.15 |
| Huadu | 7,118,958 | 0.74 |
| Nansha | 6,227,502 | 0.94 |
| Conghua | 2,232,912 | 0.11 |
| Zengcheng | 6,660,259 | 0.41 |
| Guangzhou | 44,254,689 | 0.61 |

The proportion of risk population was the highest in Huadu District (3.87%), followed by Nansha District (2.19%) and Huangpu District (1.80%), reflecting that the density of residents around high-voltage power towers in these areas was relatively high, or the coverage area of the power towers overlapped greatly with the residential areas. Yuexiu District has the lowest proportion (0.05%), while Baiyun District (0.30%) and Tianhe District (0.34%) are also at a low level, indicating that the central urban area and the densely populated Baiyun District (with the highest total population in the city) have effectively reduced the overlap rate between high-voltage power towers and densely populated areas through planning control.

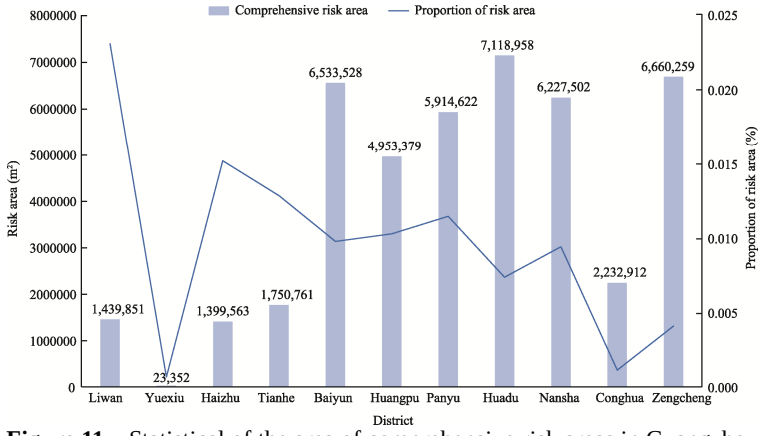


**Figure 11** Statistical of the area of comprehensive risk areas in Guangzhou

**Table 5** Statistical of the population covered by risk areas

| District | Total population (persons) | Population in risk areas (persons) | Proportion (%) |
|---|---|---|---|
| Liwan | 1,213,780 | 4,600 | 0.38 |
| Yuexiu | 1,057,678 | 544 | 0.05 |
| Haizhu | 1,823,507 | 11,081 | 0.61 |
| Tianhe | 2,238,660 | 7,660 | 0.34 |
| Baiyun | 3,737,903 | 11,179 | 0.30 |
| Huangpu | 1,269,467 | 22,878 | 1.80 |
| Panyu | 2,659,292 | 41,712 | 1.57 |
| Huadu | 1,636,056 | 63,239 | 3.87 |
| Nansha | 844,962 | 18,503 | 2.19 |
| Conghua | 717,283 | 11,222 | 1.56 |
| Zengcheng | 1,463,770 | 18,212 | 1.24 |
| Guangzhou | 18,662,358 | 210,830 | 1.13 |

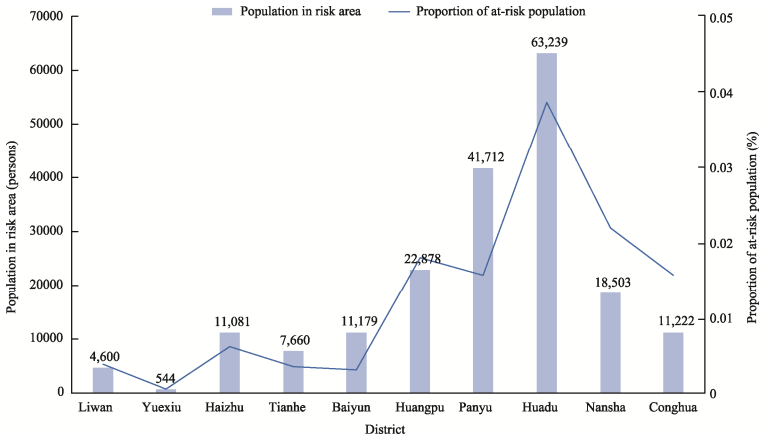


**Figure 12** Statistical of the population covered by risk areas

### **3.2.6** Calculation of the Shortest Fire Rescue Time of High-voltage Power Towers

Once a high-voltage power tower collapses or catches fire, rescue personnel need to arrive at the scene promptly. First, calculate the shortest time for the nearest fire station to reach each high-voltage power tower through the road network. 12 classes of vehicle travel roads were selected to establish a road network dataset, while the internal off-network roads were deleted. The road length was calculated, and the travel time was calculated based on the driving speed. The specific road classes and their speeds are shown in Table 6. The road data

**Table 6** Types and speeds of vehicular lanes

| Class | Name | Category | Speed (km/h) |
|---|---|---|---|
| motorway | Motorway | Elevated and express way | 100 |
| motorway_link | Link of motorway | Elevated and express way | 40 |
| trunk | Trunk road | Elevated and express way | 70 |
| trunk_link | Link of trunk road | Elevated and express way | 40 |
| primary | Primary road | Urban main trunk road | 55 |
| primary_link | Link of primary road | Urban main trunk road | 40 |
| secondary | Secondary road | Urban main trunk road | 50 |
| secondary_link | Link of secondary road | Urban main trunk road | 40 |
| tertiary | Tertiary road | Urban sub-trunk road | 45 |
| tertiary_link | Link of tertiary road | Urban sub-trunk road | 40 |
| residential | Residential road | Urban branch road | 30 |
| unclassified | Unclassified road | Urban branch road | 30 |

of OSM sets nodes at connected intersections, while there are no common nodes at three-dimensional intersections. Therefore, the connectivity of the network dataset is set to be connected to any node. Conduct a nearest facility point analysis for each high-voltage power tower, locate the nearest fire station and calculate the shortest arrival time. Considering that some high-voltage power towers may be far from the road, the distance from the high-voltage power towers to the road was converted into time at a speed of 30 km/h and included together. The final results of the shortest rescue time for each power tower are shown in Figure 13. The rescue time of each power tower is integrated into the attribute table of the high-voltage power tower. The number and proportion of high-voltage power towers in different time periods are statistically shown in Table 7. The results show that nearly half of the high-voltage power towers can receive fire rescue within 5 minutes, and over 80% of the power towers can be rescued within 10 minutes.

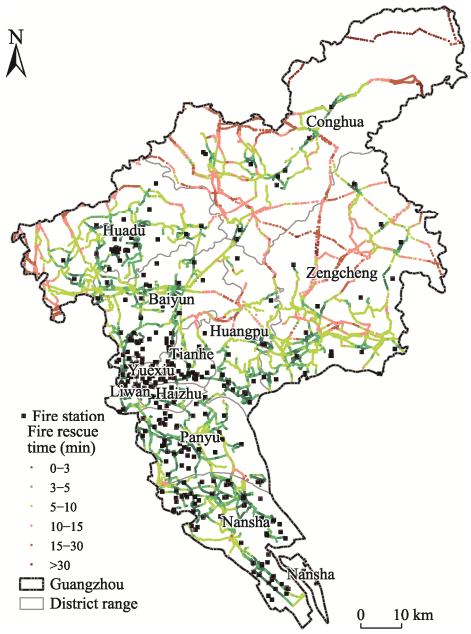


**Figure 13** Map of the shortest arrival time for fire station rescue

The rescue time for high-voltage power towers in some more remote areas is relatively long. Over a thousand power towers took more than 15 minutes to rescue, and 144 even exceeded 30 minutes. These power towers are mainly distributed in the northern part of Guangzhou City, mainly in mountainous areas. The number of fire stations is relatively small and the density is low. They are mainly concentrated in Conghua District and Zengcheng District, and in the western edge of Huadu District and the border area between Baiyun District and Huangpu District. If an accident occurs in these high-voltage power towers, the distance required for rescue will be long and the time will be considerable.

**Table 7** The number and proportion of power towers within different rescue-arriving time periods

| Time (min) | Number | Proportion (%) | Cumulative number | Cumulative proportion (%) |
|---|---|---|---|---|
| 0–3 | 3,128 | 20 | 3,128 | 20 |
| 3–5 | 3,843 | 25 | 6,971 | 45 |
| 5–10 | 5,528 | 36 | 12,499 | 81 |
| 10–15 | 1,729 | 11 | 14,228 | 92 |
| 15–30 | 1,003 | 7 | 15,231 | 99 |
| >30 | 144 | 1 | 15,375 | 100 |

### **3.2.7** Analysis of the Fire Rescue Accessibility for High-voltage Power Towers

When severe weather conditions such as thunderstorms and hail occur, the probability of multiple power towers having accidents simultaneously increases significantly. Fire station rescue operations need to respond at the same time, and the density of fire stations in different areas also varies. Therefore, from the perspective of supply and demand, we use a two-step floating catchment area method based on road network distance and Gaussian attenuation function to calculate the accessibility from a fire station to a high-voltage power tower within a certain distance. Based on the network dataset, the driving time from each fire station to each high-voltage power tower is calculated. At the same time, the time converted from the distance of the high-voltage power tower to the road network is also included as the OD cost matrix, which is used for the judgment of Gaussian attenuation and the calculation of weights. The time search thresholds for the Gaussian attenuation function were set at 5 minutes, 10 minutes, 15 minutes, and 30 minutes respectively. The calculated reachability is shown in Figure 14. Similarly, the reachability data of each power tower were

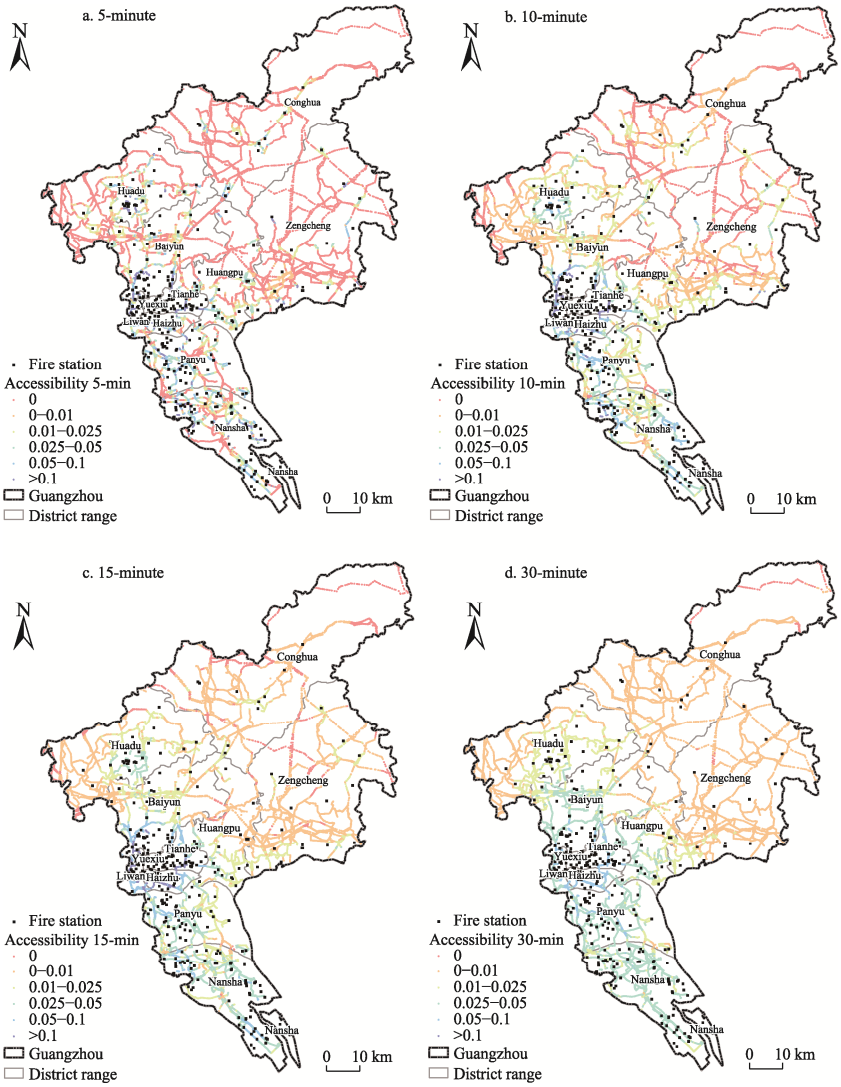


**Figure 14** Maps of the accessibility of fire stations for each power tower

integrated into the attribute table of the high-voltage power tower. The larger the value, the greater the rescue force that the fire station can allocate to this high-voltage power tower. The smaller the value, the lower the accessibility from the fire station to the high-voltage power tower. Once multiple power towers have accidents simultaneously, it becomes more difficult to allocate fire rescue. A value of 0 indicates that no fire station can reach the high-voltage power tower at this time threshold. From a spatial perspective, the density of fire stations in the central urban area of Guangzhou is relatively high, and the nearby high-voltage power towers all show good accessibility. The fire station accessibility of high-voltage power towers in the peripheral counties and districts, especially in the northeastern part of the city, is relatively poor. Except for the high-voltage power towers that are relatively close to the fire stations, once the time threshold is reduced, the fire station accessibility of a batch of high-voltage power towers will drop to 0.

The number of high-voltage power towers with different accessibility ranges under different time thresholds is statistically analyzed in Table 8. When the time threshold is 30 minutes, the accessibility of most high-voltage power towers is concentrated between 0 and 0.1 fire stations, with only 144 high-voltage power towers having no accessible fire stations. When the time threshold is set at 15 minutes, the accessibility of high-voltage power towers with high accessibility increases, while that of high-voltage power towers with low accessibility decreases. The overall change is relatively small. When the threshold was further shortened to 10 minutes, the accessibility of some high-voltage power towers exceeded 0.25, and the number of power towers that were not accessible to fire stations also increased further. When the threshold was shortened to 5 minutes, the number of power towers without fire station accessibility increased sharply. More than half of the power towers had no fire station accessibility. On the other hand, the fire station accessibility of 13 high-voltage power towers exceeded 1, with the highest value exceeding 3. Analysis shows that within a rescue time of 10 to 15 minutes, the accessibility of high-voltage power towers to fire stations is relatively balanced. If a rescue time of 5 minutes is required, the current situation of fire stations cannot well meet the needs of fire rescue.

**Table 8** The number of power towers with different accessibility ranges under different time thresholds

| Accessibility | 5 (min) | 10 (min) | 15 (min) | 30 (min) |
|---|---|---|---|---|
| 0 | 8,404 | 2,876 | 1,147 | 144 |
| 0–0.01 | 1,905 | 5,116 | 6,393 | 6,535 |
| 0.01–0.025 | 2,048 | 3,897 | 3,752 | 3,123 |
| 0.025–0.05 | 1,559 | 1,963 | 2,619 | 4,758 |
| 0.05–0.1 | 891 | 1,022 | 1,075 | 815 |
| 0.1–0.25 | 461 | 463 | 389 | 0 |
| 0.25–1 | 94 | 38 | 0 | 0 |
| >1 | 13 | 0 | 0 | 0 |

## 4 Discussion and Conclusion

Electric power infrastructure is a crucial guarantee for urban production and residents' lives. High-voltage power towers are important nodes in the electric power infrastructure network. By demarcating the risk areas around high-voltage power towers and calculating the accessibility of fire rescue, it can provide references for high-voltage power tower rescue and urban construction in megacities. Based on the basic data of high-voltage power towers, roads, buildings, fire stations, etc., researchers have proposed a spatial analysis method for the risk areas and rescue accessibility of high-voltage power towers. The analysis idea is to take high-voltage power towers as the main data object, integrate relevant multi-source data, construct road-near and building-near risk areas, and statistically analyze the population in

the risk areas. Finally, calculate the rescue time for the high-voltage power tower and the accessibility within different rescue times.

Taking Guangzhou City as an example, the researchers illustrated the spatial analysis process of the risk areas and rescue accessibility of high-voltage power towers, and proposed corresponding spatial analysis methods. The results of the analysis on the adjacent risk areas and rescue accessibility of high-voltage power towers mainly show: (1) In the central urban area and the central region, there are many risk areas for high-voltage power towers that are combined road-near and building-near, while in the northern mountainous areas, the risk areas for high-voltage power towers are mainly road-near. (2) Most high-voltage power towers can be rescued within 10 minutes, while the rescue time for some high-voltage power towers in remote areas is longer. (3) High-voltage power towers in areas with high fire station density all show good accessibility to fire stations, while those in peripheral counties and districts that are far from fire stations have poorer accessibility to fire stations, and the above manifestations become more obvious as the time threshold decreases.

Due to the limitations of the corresponding conditions, there may be certain deviations and omissions in the researchers' exploration and statistics of the spatial distribution of high-voltage power towers and risk areas. If more accurate data is needed, it should be combined with more detailed field investigations. In the future, at the macro level, it is necessary to expand the research scope and combine new technologies such as artificial intelligence remote sensing interpretation to establish large-scale datasets for the risk areas and rescue accessibility of high-voltage power towers. At the micro level, it is necessary to analyze more accurate high-voltage power towers and related spatial data, and explore the mechanisms behind spatial laws by combining local spatial characteristics.

### *Author Contributions*

Liu, C. collected the spatial data, and wrote the manuscript; Yang, Y. and Li, S. J. did the data validation, and designed the method; He, Y. L. and Yang, Z. processed the spatial data, and wrote part of the data paper; Wang, S. H. reviewed, supervised, edited, and improved the paper.

### *Conflicts of Interest*

The authors declare no conflicts of interest.

## References

[1] Tao, B. Q., Wang, C., Qu, H. Y., *et al*. Design of U-shaped high-voltage transmission line wireless power transfer system based on vertical relay [J]. *Electrical Measurement & Instrumentation*, 2024, 61(3): 217–224. DOI: 10.19753/j.issn1001-1390.2024.03.030.

[2] United Nations. The sustainable development goals report 2024 [R]. New York: United Nations, 2024.

[3] Yang, Y. Energy globalization of China: interaction logic and spatial transition [J]. *Acta Geographica Sinica*, 2022, 77(2): 295–314. https://doi.org/10.11821/dlxb202202003.

[4] Arderne, C., Zorn, C., Nicolas, C., *et al*. Predictive mapping of the global power system using open data [J]. *Scientific data*, 2020, 7(1): 19.

[5] Wu, H. P., Wang, L. X., Cheng, X., *et al*. Important evaluation of nodes of lifeline system based on network analysis: take the power grid in some districts of Guangzhou City as an example [J]. *Earthquake Engineering and Engineering Dynamics*, 2015, 35(6): 232–238. DOI: 10.13197/j.eeev.2015.06.232.wuhp.032.

[6] Jiang, S. Y., Pan, C. P., Zhuang, Z. W., *et al*. Analysis of collapse accident of transmission line tower causing by typhoon attacking in the coastal district of Guangdong Province [J]. *Southern Energy Construction*, 2016, 3(S1): 82–87. DOI: 10.16516/j.gedi.issn2095-8676.2016.S1.018.

[7] Vettoretto, G., Li, Z., Affolter, C. Evaluation of the ultimate collapse load of a high-voltage transmission tower under excessive wind loads [J]. *Buildings*, 2023, 13(2): 513.

[8] Li, G. F. Foundation reinforcement technology of high voltage electric tower in typical limestone stratum in Guangzhou Area [J]. *Chinese & Overseas Architecture*, 2019(10): 153–157. DOI: 10.19940/j.cnki.1008-0422.2019.10.044.

[9] Shu, H. K., Luo, W. Z. Analysis on the effect of mining method in tunnel construction on the neighbor electricity pylon [J]. *Engineering Construction*, 2019, 51(3): 9–13. DOI: 10.13402/j.gcjs.2019.03.002.
[10] Yang, S., Hu, B., Zhou, B. J., *et al*. Power line aerial image restoration under adverse weather: datasets and baselines [J]. *IEEE Journal of Selected Topics in Applied Earth Observations and Remote Sensing*, 2025, 18: 10105–10119.
[11] Li, X. L., Yang, S. Q., Yao, J., *et al*. Research on extraction method of transmission line high-voltage tower based on laser point cloud data [J]. *Electrical Engineering Materials*, 2025(1): 70–73. DOI: 10.16786/j.cnki.1671-8887.eem.2025.01.016.
[12] Cheng, X. F. Stability analysis and protection design of road slopes involving high-voltage power towers [J]. *Transport Business China*, 2022(16): 17–19.
[13] Zhang, R. Z. Safety assessment of power transmission corridors in forestry area based on multi-source data [D]. Wuhan: Wuhan University, 2020. DOI: 10.27379/d.cnki.gwhdu.2020.000768.
[14] Wang, Y. X., Han, Y. Measuring maritime search and rescue (SAR) accessibility using an improved spatiotemporal two-step floating catchment area method: a case study in the South China Sea [J]. *Journal of Transport Geography*, 2025, 124: 104155.
[15] Wu, D., Tie, X., Li, C., *et al*. An extremely low visibility event over the Guangzhou region: a case study [J]. *Atmospheric Environment*, 2005, 39(35): 6568–6577.
[16] Zhong, E. S. Deep mapping: a critical engagement of cartography with neuroscience [J]. *Geomatics and Information Science of Wuhan University*, 2022, 47(12): 1988–2002. DOI: 10.13203/j.whugis20220382.
[17] Guo, R. Z. Spatial analysis (Second edition) [M]. Beijing: Higher Education Press, 2001.
[18] Staniek, M., Schumann, R., Züfle, M., *et al*. Text-to-overpassql: a natural language interface for complex geodata querying of openstreetmap [J]. *Transactions of the Association for Computational Linguistics*, 2024, 12: 562–575.
[19] Zhang, Y. C., Zhao, H. M., Long, Y. CMAB: a multi-attribute building dataset of China [J]. *Scientific Data*, 2025, 12: 430.
[20] Chen, Y. H., Xu, C. C., Ge, Y., *et al*. A 100 m gridded population dataset of China's seventh census using ensemble learning and big geospatial data [J]. *Earth System Science Data*, 2024, 16(8): 3705–3718.
[21] Xiang, W. N. GIS-based riparian buffer analysis: injecting geographic information into landscape planning [J]. *Landscape and Urban Planning*, 1996, 34(1): 1–10.
[22] Ma, M. Y., Wu, Y., Luo, W. Z., *et al*. HiBuffer: buffer analysis of 10-million-scale spatial data in real time [J]. *ISPRS International Journal of Geo-Information*, 2018, 7(12): 467.
[23] Zhang, W. Y. GIS buffer and overlay analysis [D]. Changsha: Central South University, 2007.
[24] Mao, D. S. Algorithm study of vector data overlaying analysis based on computational geometry [D]. Jinan: Shandong University of Science and Technology, 2007.
[25] Ali, M. I., Abidin, M. R. Population density and intensity of traffic connection: spatial analysis (overlay) [J]. *International Journal of Science and Research*, 2018, 7: 546–552.
[26] Chen, Y., Jin, F. J., Lu, Y. Q., *et al*. Development history and accessibility evolution of land transportation network in Beijing-Tianjin-Hebei Region over the past century [J]. *Journal of Geographical Sciences*, 2018, 28(10): 1500–1518.
[27] Ashik, F. R., Islam, M. S., Alam, M. S., *et al*. Dynamic equity in urban amenities distribution: an accessibility-driven assessment [J]. *Applied Geography*, 2024, 164: 103199.
[28] Ye, P., Ye, Z. Q., Xia, J. Z., *et al*. National-scale 1-km maps of hospital travel time and hospital accessibility in China [J]. *Scientific Data*, 2024, 11(1): 1130.
[29] Zhang, H. Hierarchical analysis and expression of urban road network based on complex network: taking Jinan and Beijing as examples [D]. Beijing: China University of Geosciences (Beijing), 2021. DOI: 10.27493/d.cnki.gzdzy.2021.000225.
[30] Zhu, Y. Y., Yang, Y., Li, J. J., *et al*. Research on the spatial pattern of the public cultural services in Wuhan City [J]. *Journal of Central China Normal University (Natural Sciences)*, 2017, 51(4): 526–533. DOI: 10.19603/j.cnki.1000-1190.2017.04.018.
[31] Luo, W., Wang, F. H. Measures of spatial accessibility to health care in a GIS environment: synthesis and a case study in the Chicago Region [J]. *Environment and Planning B*, 2003, 30(6): 865–884.
[32] Wei, Y., Xiu, C. L., Gao, R., *et al*. Evaluation of green space accessibility of Shenyang using Gaussian based 2-step floating catchment area method [J]. *Progress in Geography*, 2014, 33(4): 479–487.
[33] Tong, D., Sun, Y. Y., Xie, M. M. Evaluation of green space accessibility based on improved Gaussian two-step floating catchment area method: a case study of Shenzhen City, China [J]. *Progress in Geography*, 2021, 40(7): 1113–1126.